

This discussion paper is/has been under review for the journal Biogeosciences (BG).  
Please refer to the corresponding final paper in BG if available.

# The role of tectonic uplift, climate and vegetation in the long-term terrestrial phosphorous cycle

C. Buendía<sup>1</sup>, A. Kleidon<sup>1</sup>, and A. Porporato<sup>2</sup>

<sup>1</sup>Max Planck Institut für Biogeochemie, P.O. Box 10 01 64, 07701 Jena, Germany

<sup>2</sup>Department of Civil Environmental Engineering, Duke University, Durham, NC 27708, USA

Received: 23 December 2009 – Accepted: 1 January 2010 – Published: 14 January 2010

Correspondence to: C. Buendía (cbuendia@bgc.pmg-jena.de)

Published by Copernicus Publications on behalf of the European Geosciences Union.

301

## Abstract

Phosphorus (P) is a crucial element for life and therefore for maintaining ecosystem productivity. Its local availability to the terrestrial biosphere results from the interaction between climate, tectonic uplift, atmospheric transport and biotic cycling. Here we present a mathematical model that describes the terrestrial P-cycle in a simple but comprehensive way. The resulting dynamical system can be solved analytically for steady-state conditions, allowing us to test the sensitivity of the P-availability to the key parameters and processes. Given constant inputs, we find that humid ecosystems exhibit lower P availability due to higher runoff and losses, and that tectonic uplift is a fundamental constraint. In particular, we find that in humid ecosystems the biotic cycling seems essential to maintain long-term P-availability. The time-dependent P dynamics for the Franz Josef and Hawaii chronosequences show how tectonic uplift is an important constraint on ecosystem productivity, while hydroclimatic conditions control the P-losses and speed towards steady-state. The model also helps describe how with limited uplift and atmospheric input, as in the case of the Amazon Basin, ecosystems must rely on mechanisms that enhance P-availability and retention. Our analysis underlines the need to include the P cycle in global vegetation-atmosphere models for a reliable representation of the response of the terrestrial biosphere to global change.


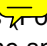
## 1 Motivation


Phosphorus (P) is a particularly important element for life. At small-scales, it serves as the driver of cellular energy cycles and is also responsible for building the molecules DNA and RNA. At larger scales, ecosystem productivity is often constrained by the availability of P (Chadwick et al., 1999; Walker and Syers, 1976; Wardle, 2004; Wardle et al., 2009; Crews et al., 1995). In contrast to other macronutrients (e.g., nitrogen), once released from its geologic source, P is quickly converted into less available forms or is removed from the land system by erosion and percolation (Walker and Syers,


302

1976; Brady and Weil, 2008). In the context of abiotically controlled processes, the P-cycle is closed on geologic time scales (ca. 1 million years) by uplift of fresh material to the soil. Therefore, alterations to the P-cycle could have long-lasting consequences (Brady and Weil, 2008). Embedded within this slow cycle, P is cycled relatively quickly  
5 between the soil and vegetation. This delicate balance of the P-cycle is well known within the agricultural and environmental engineering context: an insufficient P supply quickly causes vegetation stress, while excessive fertilization quickly contributes to groundwater and stream flow contamination (Brady and Weil, 2008).

Soil formation and P limitation is studied using data obtain from chronosequences. A  
10 chronosequence is "a sequence of soil developed on similar parent materials and relief under the influence of constant or ineffectively varying climate and biotic factors, whose differences can thus be ascribed to the lapse of differing increments of time since the initiation of the soil formation" (Stevens and Walker, 1970). Chronosequences start after catastrophic phenomena such as volcanic activity, floods, or glaciation (Stevens  
15 and Walker, 1970) which restarts the soil formation. Thus in these cases the age of the soil is approximately known, and the use of chronosequence data is useful to understand the transient dynamics of the P-cycle in the absence of exogenous inputs and appreciable soil regeneration mechanisms. Based on chronosequence data Walker and Syers (1976) proposed a conceptual model to explain the depletion of terrestrial  
20 phosphorus, outlining the importance of exogenous inputs for the productivity of some ecosystems on old soils. However, most of the terrestrial productivity occurs in soils that refresh continuously due to the action of tectonic and isostatic uplift and in the presence of exogenous P inputs.

To shed light on this aspect, Porder et al. (2007) developed a model that accounts  
25 for uplift by assuming a steady-state in which uplift equals erosion. They showed that for areas with moderate uplift rates, P depletion is unlikely, but in areas with slow uplift rates,  the Amazon Basin, ecosystems will depend more strongly on exogenous inputs  Porder et al., 2007). Conversely, Mahowald et al. (2005, 2008), have shown that the amount of aerosol particles containing P leaving the Amazon Basin is greater

than the input with a net loss through the atmosphere of  $1.3 \text{ mg P m}^{-2} \text{ a}^{-1}$ , illustrating our lack of understand about the P budget of this ecosystem. While in reference to the Hawaiian Islands, it was shown that the dust particles coming from Continental Asia contributed to the productivity on the islands once the P in fresh volcanic rock  
5 was depleted (Chadwick et al., 1999). Other P-sources, such as guano deposition by seabird colonies were also shown to be important in  cases (Wardle et al., 2009). In this regard, it is interesting to note that some ancient cultures already considered guano to be of great importance to terrestrial productivity (e.g., during the Inca empire disturbing sea-bird colonies on the pacific coast was punished with death (Hughes,  
10 1999)). On the one hand, given the inherent difficulty in monitoring soil biogeochemical cycles at a sufficiently precise spatial and temporal resolution, numerical models have been commonly used to analyze the role of different processes in maintaining stable P cycling and thus ecosystem productivity, as well as to understand to what extent terrestrial productivity may feed back on the  $\text{CO}_2$  concentration and climate change  
15 (Cramer et al., 2001). However, these studies have been criticized for overestimating both future terrestrial carbon sequestration and the potential carbon climate feedback because they do not account for nutrient constraints (Hungate et al., 2003). There are now models that account for the N constraint (e.g., Zaehle et al., 2010), but the predictions for the tropics are uncertain because these ecosystems are often P limited  
20 (Crews et al., 1995).

On the other hand, extracting the dominant processes responsible for the long-term biogeochemical interactions may be difficult in these complex models, which typically involve an extremely large number of parameters and degrees of freedom and where the results are necessarily numerical. In this regard, simplified analytical models provide a useful alternative, especially when cast in the fo  of systems of ordinary differential equations (Manzoni et al., 2004; Lasaga, 1980), for which the apparatus of stability and bifurcation analyses typical of dynamical system theory becomes readily available (e.g., Strogatz, 1994). With this intent, here we propose a simple analytical P-cycle model valid at long temporal (decades and higher) and large spatial (regional

to continental) scales, with the aim of clarifying how tectonic uplift, climate, vegetation, and exogenous inputs interact to maintain the active P-cycle in terrestrial ecosystems under different hydroclimatic conditions. Given its simplicity, the model can be easily coupled to other models of biogeochemical cycles, or be used to initialize the phosphorus pools of more complex models running on daily or sub-daily time-scales.

In the following, we will describe the P-cycle and how we model it. We then calculate the steady-state for ecosystems without uplift (e.g., volcanic islands such as Hawaii), as well as for ecosystems with constant uplift (e.g., tectonic uplift and isostatic rebound as in the Amazon Basin). Using the steady-state solutions, we evaluate how P availability in terrestrial ecosystems is affected by a) reduction of organic biomass losses, b) active P uptake by vegetation and c) the input of P by animals. Finally, the implications of these processes are discussed in the context of Hawaii, New Zealand and the Amazon Basin using the time-dependent solution of our model.

## 2 Model formulation

We formulate our model based on the schematic P-cycle representation of Fig. 1. Symbols and units are summarized in Table 1, with Table 2 providing an explanation of the parameters. Possible ranges of the inputs, fluxes and pools are included in Fig. 1. Our model considers the average vertical content of P throughout the soil layer.

### 2.1 Synthesis of the P-cycle model

Phosphorus has a very slow geochemical cycle driven mainly by tectonic processes. The uplift of primary material ( $I_w$ ) is the primary input to the land system. Weathering ( $F_{wd}$ ) is the next step where primary mineral phosphorus ( $P_w$ ), normally in the form of apatite, is transformed into a dissolved phosphate form ( $P_d$ ). Within this phase, aluminum, manganese and iron are released from primary mineral sources during weathering ( $F_{wm}$ ). These ions stay in the soil to form secondary minerals or clays ( $M_m$ ).

305

These secondary minerals can absorb phosphate in soil solution ( $P_d$ ) to form bonded P compounds ( $P_c$ ) that are almost insoluble, acting as a sink of P in the system. As weathering takes place, secondary minerals form, resulting in old soils having a greater P-retention capacity (Brady and Weil, 2008). P in soil solution is taken up by vegetation ( $F_{pv}$ ), either passively with root water uptake, or actively by osmotic adjustments in roots. In plants, with the synthesis of organic matter, P becomes part of vegetation biomass ( $P_v$ ). Litter fall then releases P back into the soil ( $F_{vo}$ ), as soil organic matter ( $P_o$ ), in forms bound to carbon and nitrogen. After mineralization ( $F_{od}$ ), P again becomes available to vegetation.

### 2.2 Climatic forcing

We investigate different climate regimes in the context of differences in mean soil moisture and temperature. Soil moisture content drives the dynamics of several biogeochemical fluxes, including mineralization, leaching and plant uptake (Porporato et al., 2003). The long-term relative soil moisture content,  $s$ , determined by the average water balance, is assumed to vary here from 0.2 in dry regions to 0.8–0.9 in very wet regions. The soil water content per unit ground area over a rooting depth of  $Z_r$  is given by  $nZ_r s$ , where  $n$  is soil porosity.

### 2.3 Inputs

#### 2.3.1 Atmospheric transport and input from animals

The atmosphere can transport phosphorus in the form of small particles for thousands of kilometers. Those particles (ashes, dust or biogenic) affect the local P budget. Possible annual ranges vary from 0.0007 to 0.1 g P m<sup>-2</sup> (Newman, 1995). At the local scale, animals can also be an important P source accounting not only for the redistribution of nutrients on land, but also returning P from the ocean or fresh water ecosystem to land (Wardle et al., 2009). Although it is difficult to estimate the animal input to ecosystems,

306

we include it in the model in order to explore its potential importance in some ecosystems (Wardle et al., 2009). We refer to the sum of those two inputs as dissolvable input  $I_d$  and assume that by these inputs P enters directly into the dissolved pool. We also refer to  $I_d$  as the exogenous input.

### 5 2.3.2 Input by tectonic and isostatic uplift

The uplift of metamorphic, sedimentary, and igneous rocks to the land surface marks the beginning of the phosphorus cycle. The amount of P in the fresh rock entering the soil profile driven by tectonic and isostatic uplift is expressed in the model as  $I_w$ . We use this parameter to compare different tectonic configurations as suggested by Porder et al. (2007), who accounted for this input by considering the local uplift rates and P concentration in primary mineral. Typically, uplift can range from 0 to approximately 8 m per thousand years (Porder et al., 2007).

## 2.4 Ecosystem internal fluxes

### 2.4.1 Phosphorus weathering

15 Once the P-containing rock enters the root zone, it is more easily chemically and physically weathered ( $F_{wd}$ ). Since weathering of one mole of apatite requires four mols of  $CO_2$  and three moles of  $H_2O$ , and  $CO_2$  is normally found in non-limiting concentrations, it is reasonable to assume that in the reaction, water and apatite concentrations are the limiting components (Chameides and Perdue, 1997). Moreover, chemical weathering  
20 occurs faster in warm environments, while physical weathering may occur faster in cold, seasonally-variable environments (Brady and Weil, 2008). For simplicity, we will assume that these effects balance out and neglect the role of temperature as the main weathering driver. As a result, weathering is modeled as

$$F_{wd} = k_w f_w(s) P_w, \quad (1)$$

307

where  $f_w(s)$  is a function of soil moisture and  $k_w$  is a reaction at a constant rate independent of temperature.

### 2.4.2 Formation of secondary minerals and P occlusion

During soil development, Al, Mn, Fe, and P compounds found in the rocks are released  
5 into the soil by weathering. Al, Fe, and Mn differ from P in that they tend to form secondary minerals. The occlusion of P by clays containing Al, Fe, and Mn is considered to be an important sink of P and therefore, although our model strives to be simple, we introduce a pool of secondary minerals  $M_m$ , to account for the phosphorus retention capacity of the soil. This pool represents an important difference to the model of Porder  
10 et al. (2007).

To derive the rate of weathering and later formation of this secondary mineral, we simply assume it to be proportional to phosphorus weathering

$$F_{wm} = k_m F_{wd} \quad (2)$$

where  $k_m$  represents the secondary mineral formation to P weathering ratio. Occlusion  
15 or fixation of phosphorus in  $M_m$  ( $F_{dc}$ ) is proportional to the amount of P in dissolved form ( $P_d$ ) and the amount of  $M_m$ , that is

$$F_{dc} = k_c P_d M_m \quad (3)$$

where  $k_c$  is a parameter that can be adjusted to obtain realistic occlusion rates. While  
20 some soils can occlude as much as  $240 \text{ g P m}^{-2}$ , soils with occlusion of  $70 \text{ g P m}^{-2}$  are still considered high P occluding soils (Brady and Weil, 2008).

### 2.4.3 Vegetation P-uptake and litter fall

We assume that the uptake of P by vegetation is proportional to the transpiration rate  
 $T(s)$  (Porporato et al., 2003), which is in turn assumed to be linearly related to relative

308

soil moisture,

$$F_{dv} = k_u T(s) \frac{P_d}{nZ_r s} \quad (4)$$

where  $T(s) = s\eta$  assuming a maximum transpiration rate  $\eta = 5 \text{ mm d}^{-1}$ , and with  $k_u$  accounting for the role of diffusion and mycorrhizae hyphae in the movement of the phosphate ions to plant roots (Brady and Weil, 2008). Across terrestrial ecosystems, the carbon to phosphorus molar ratio ranges in foliage from 900 in temperate regions to 2450 in tropical regions with typical litterfall molar ratios from about 1700 in temperate regions to 4100 in tropical regions (McGroddy et al., 2004; Manzoni et al., 2010). We therefore do not assume a constant C to P ratio in plants. The amount of P lost from vegetation by litter fall ( $F_{vo}$ ) is described as a fractional loss per year ( $k_p$ ) of total P in the vegetation,

$$F_{vo} = k_p P_v \quad (5)$$

#### 2.4.4 P-mineralization

Phosphorus mineralization ( $F_{od}$ ) is the transformation of organic P in soil organic matter ( $P_o$ ) to mineral phosphorus,  $P_d$ . Organic matter decomposition is a process driven by soil microbes, whose rate of activity in turn, depends on soil moisture ( $s$ ) and temperature ( $T$ ) (Porporato et al., 2003). Assuming first order kinetics, we express mineralization as

$$F_{od} = k_d f(s, T) P_o \quad (6)$$

where decomposition increase with soil moisture and temperature.

309

## 2.5 Losses

Leakage and runoff ( $LQ(s)$ ) is a nonlinear function of soil moisture (e.g., Rodriguez-Iturbe and Porporato, 2004) represented by

$$LQ(s) = k_l s^c \quad (7)$$

where  $k_l$  accounts for the runoff-leakage rate at saturation. Phosphorus is lost from the system by surface runoff, drainage, erosion, fire and anthropogenic removal. Losses from the dissolved P pool ( $O_d$ ) are mainly driven by runoff and deep infiltration,  $LQ(s)$ , and are proportional to the total concentration of  $P_d$

$$O_d = LQ(s) \frac{P_d}{nZ_r s} \quad (8)$$

Losses of organic matter from the system are in part assumed to be linked to water losses, but a separate term,  $k_f$ , is used to account for the losses by natural processes (e.g., glaciation and wind erosion), and induced losses as a result of human activity (e.g., fires and biomass removal) (Brady and Weil, 2008; Mahowald et al., 2005). As a result, the external P-losses from the soil organic matter pool are

$$O_o = (k_r LQ(s) + k_f) P_o \quad (9)$$

We also account for erosion, subsidence, and lateral losses of secondary minerals ( $O_m$ ) and occluded P ( $O_c$ ). For simplicity, these are described using a constant rate  $k_e$

$$O_m = k_e M_m \quad (10)$$

and

$$O_c = k_e P_c \quad (11)$$

310

## 2.6 P-balance equations

The following ordinary differential equations describe the dynamics of the five P pools, plus the secondary mineral pool (Fig. 1). The primary mineral P in the soil profile ( $P_w$ ) increases with the uplift process ( $I_w$ ) and decreases as weathering reactions take place

5  $F_{wd}$  (described in Eq. 1),

$$\frac{dP_w}{dt} = I_w - F_{wd} \quad (12)$$

The amount of secondary minerals increases by weathering  $F_{wm}$  (Eq. 2) and decreases by erosion, subsidence and lateral losses  $O_m$  (Eq. 10)

$$\frac{dM_m}{dt} = F_{wm} - O_m \quad (13)$$

10 We describe the dynamics of the occluded P pool ( $P_c$ ) by accounting for occlusion ( $F_{dc}$ ), a non-linear term that depends on the size of the secondary mineral pool and the amount of P in soil solution (Eq. 3). Since de-occlusion of P only seems to play an important role in early soil formation states, we account only for losses related to erosion processes  $O_c$  (refer to Eq. 11)

$$15 \frac{dP_c}{dt} = F_{dc} - O_c \quad (14)$$

The dynamics of the P pool in vegetation ( $P_v$ ) is determined by the balance between P uptake  $F_{dv}$  (Eq. 4) and litter fall ( $F_{vo}$ ) (Eq. 5)

$$\frac{dP_v}{dt} = F_{dv} - F_{vo} \quad (15)$$

20 We describe the dynamics of P in the soil organic matter as the result of the balance between the input from vegetation litter  $F_{vo}$  (Eq. 5), the losses from mineralization  $F_{od}$  (Eq. 6) and losses due to fire, erosion and water runoff  $F_{ov}$  (Eq. 9)

$$\frac{dP_o}{dt} = F_{vo} - F_{od} - O_o \quad (16)$$

311

The P in soil solution ( $P_d$ ) bridges the decomposition, weathering, external losses and occlusion. The three inputs to this pool are, exogenous inputs  $I_d$ , mineralization  $F_{od}$  (Eq. 6) and weathering  $F_{wd}$  (Eq. 1). Vegetation uptake  $F_{dv}$  (Eq. 4), occlusion in secondary minerals  $F_{dc}$  (Eq. 3) and the runoff and leakage  $O_d$  (Eq. 8) account for the P

5 losses

$$\frac{dP_d}{dt} = I_d + F_{wd} + F_{od} - (F_{dv} + F_{dc} + O_d) \quad (17)$$

where  $F_{dc}$  is a non-linear term (Eq. 3).

## 3 Results

10 We evaluate the role of tectonic uplift and the implication of the ecological processes in the context of the P-cycle across different climates. Because of the model simplicity and few nonlinearities, it is actually possible to analytically obtain the general steady-state solution of the system. We are then able to perform a sensitivity analysis of the main parameters as well as an analysis of the relative roles of the inputs and climate forcing.

### 3.1 Steady-state solution

15 The steady-state solutions are obtained by setting the time derivatives of the phosphorus cycle (Eqs. 12–17) to zero. The corresponding solutions, indicated with a hat, are obtained in closed form as

$$\hat{P}_w = \frac{I_w}{k_w \cdot f_w(s)} \quad (18)$$

$$20 \hat{M}_m = \frac{k_m I_w}{k_e} \quad (19)$$

312

$$\hat{P}_c = \frac{k_c \hat{P}_d \hat{M}_m}{k_e^2} \quad (20)$$

$$\hat{P}_o = \frac{k_v \hat{P}_v}{k_d f(s, T) + k_f + k_r LQ(s)} \quad (21)$$

$$\hat{P}_v = \frac{T(s) \hat{P}_d}{k_v n Z_r s} \quad (22)$$

$$\hat{P}_d = \frac{(I_d + I_w) k_e n Z_r s (k_d f(s, T) + k_r LQ(s) + k_f)}{k_d f(s, T) (k_e LQ(s) + k_c k_m I_w n Z_r s) + (k_f + k_r LQ(s)) (k_c k_m I_w n Z_r s + k_e LQ(s) + T(s))} \quad (23)$$

- 5 We then analyze the solution as a function of soil moisture ( $s$ ), uplift ( $I_w$ ), exogenous inputs ( $I_d$ ).

### 3.1.1 Sensitivity of ecosystems external inputs to soil moisture

Changes in the rainfall regime alter soil moisture which in turn affects weathering, runoff, vegetation water uptake and mineralization of organic matter. Figure 2 shows the steady-state of ecosystems under different soil moisture conditions, from very dry ( $s = 0.2$ ) to very wet ( $s = 0.8$ ). The effects of soil moisture changes are analyzed for the three different forms of input, keeping the total input constant ( $I_d + I_w = 0.018 \text{ g P m}^{-2} \text{ a}^{-1}$ ).

By comparing the three different types of inputs in Fig. 2, we observe differences in the amount of P in primary minerals (Fig. 2a), the P retention capacity (Fig. 2b), and the P in occluded form (Fig. 2c). Occlusion does not have a large influence on the P dissolved pool (Fig. 2d). The organic, dissolved, and vegetation P pools are very similar for the three types of input, although weathering was defined as a function of soil moisture (Eq. 1). We would therefore expect greater P weathering in wet regions. However,

313

for systems in steady-state, weathering becomes independent of soil moisture, as can be seen from the solution,

$$F_{wd} = F_{wd} = k_w f_w(s) \hat{P}_w = k_w f_w(s) \left( \frac{I_w}{k_w \cdot f_w(s)} \right) = I_w \quad (24)$$

This is due to dry regions having more material to be weathered (ca.  $300 \text{ g P m}^{-2}$  more in Fig. 2a), but less moisture ( $s = 0.25$ ), while humid places have less material to be weathered but more moisture ( $s = 0.7$ ). Soil types data shows in general the same patterns (see in Okin et al., 2004, Fig. 1 bottom for the estimated soil P concentration in the top 20 cm). Moreover, due to water-related losses, we observe a generalized P-depletion in humid ecosystems. The concentration of P in the first 20 cm of the soil in dry regions (Aridisols  $92.8 \text{ g m}^{-2}$ ) tends to be higher than in wet regions (Oxisols  $35.4 \text{ g m}^{-2}$ ) (Okin et al., 2004). Our model successfully represents this pattern.

Although there is an increasing concentration of P in soil organic matter with ecosystem dryness (Fig. 2f), mineralization increases with soil moisture, leading to a peak in the mineralization rate at intermediate soil moisture. This results in the dissolved pool (Fig. 2d) having a maximum at about  $s = 0.6$ . The biotic fluxes ( $F_{dv}$ ,  $F_{vo}$  and  $F_{od}$ ) are larger with the size of the dissolved pool determined mainly by mineralization.

### 3.1.2 Sensitivity of organic biomass losses to soil moisture

Natural ecosystems have less P losses from organic biomass, than agricultural systems (Brady and Weil, 2008). Processes such as fire, herbivory and intensive rain events drive losses of organic P from the system. Figure 3 shows the sensitivity of three forms of organic matter losses to soil moisture.  $k_r$  represents systems with organic losses mainly driven by water  $O_o = (0.5k_f + 5k_r LQ(s))P_o$ , that results in the accumulation of P in dry regions. However, in dry regions wind erosion plays an important role by removing soil and biomass (Artaxo and Hansson, 1994). At the other extreme,  $k_f$  representing systems with organic matter losses mainly independently from water losses using a constant rate  $O_o = (5k_f + 0.5k_r LQ(s))P_o$ . We observe in this case that  $P_v$

314



increases with soil moisture. A combination of the two:  $O_o = (k_r LQ(s) + k_f)P_o$  gives values in the acceptable ranges of 10–25 g P m<sup>-2</sup> for  $P_o$  and 20–40 g P m<sup>-2</sup> for  $P_v$  (Brady and Weil, 2008).

### 3.1.3 Sensitivity of active P uptake by vegetation to soil moisture

- 5 Symbiosis between plants and mycorrhizae are very common, especially in ecosystems with low  $P_d$  concentrations (Brady and Weil, 2008). Figure 4 illustrates the sensitivity of active P uptake to soil moisture. Ecosystems that do not invest in symbiotic relations will have more P occluded, and also more dissolved P. Increasing active uptake minimizes the losses of P in the system, leading to higher P concentrations in  
 10 vegetation and in soil organic matter. This mechanism illustrates how particularly mid ecosystems with low P input can reduce P losses to clays and also to leaching. In the long term, this helps the ecosystem cope with low P inputs from the atmosphere and weathering.

### 3.1.4 Special solutions for systems without uplift

- 15 As previously mentioned, a system without uplift and exposed to erosion and weathering reaches a non-trivial steady-state only in the presence of exogenous inputs (Walker and Syers, 1976). In this special case, the solution simplifies into

$$\hat{P}_w = 0 \quad (25)$$

$$\hat{M}_m = 0 \quad (26)$$

20  $\hat{P}_c = 0 \quad (27)$

$$\hat{P}_o = \frac{k_v \hat{P}_v}{k_d f(s, T) + k_f + k_r LQ(s)} \quad (28)$$

$$\hat{P}_v = \frac{T(s) \hat{P}_d}{k_v} \quad (29)$$

315

$$\hat{P}_d = \frac{I_d n Z_r s (k_d f(s, T) + k_r LQ(s))}{(LQ(s) + T(s))(k_f + k_r LQ(s)) + k_d f(s, T) LQ(s)} \quad (30)$$

- When ecosystems without tectonic uplift reach their steady state, soil processes no longer play an important role. However, the largest terrestrial productivity occurs on continental crust, which even in steady-state, depends on the soil processes (fresh  
 5 material input and occlusion). Since the concept of chronosequences in the usual sense does not account for uplift, the evolution of such soils cannot be assessed with data.

## 3.2 Phosphorus temporal dynamics

- Since we cannot assume that all the terrestrial ecosystems reach their steady-state  
 10 with respect to the P cycle, in the following we discuss how the system changes in time and how such changes are related to soil moisture. In particular, we show how the transient solution of our model reproduces the dynamics of the classical conceptual model for the P cycle of Walker and Syers (1976) and the Franz Josef chronosequence. We then qualitatively compare our model results to the Hawaii chronosequence data  
 15 (Crews et al., 1995). In the Crews et al. (1995) chronosequence of Hawaii, the soil development started shortly after the formation of the volcanic island, while in the chronosequence considered by Walker and Syers in New Zealand, the soil development starts shortly after the retreat of the Franz Josef glacier. Both systems feature negligible uplift while being subject to erosion losses. To contrast this behavior, we  
 20 consider the case of the Amazon Basin, where the situation is represented by slow constant uplift rates. The time dependent solutions are calculated using a standard numerical integration of the model (Eqs. 12–17).

- The parameters in Table 2 are given assuming ecosystems can actively reduce the losses by: a) reduction of organic biomass losses, b) active P uptake by vegetation,  
 25 and c) animal inputs.

316



### 3.2.1 The Walker and Syers' model for New Zealand

The Franz Josef glacial area is located on the west side of New Zealand's Southern Island, which was formed during the collision of the Pacific and Australia continental plates during the late Cenozoic (Tippett and Kamp, 2003). Glaciers removed the soil layer, and the soil formation re-started after the glacial retreat. If one only considers the soil after the glacial retreat, the further uplift input may be assumed to be negligible (the main parameters for this systems are reported in Table 3). Walker and Syers developed a conceptual model for phosphorus based on data from the Franz Josef glacial retreat chronosequence.

We assume a mean annual atmospheric input of  $0.01 \text{ g P m}^{-2}$ , an initial pool of primary mineral P of  $38 \text{ mol P m}^{-2}$  (Porder et al., 2007) and assume that 50% of that pool can be weathered. We only assume atmospheric input for this case. With these data, the temporal dynamics of our model reproduces well the behavior of Walker and Syers' conceptual model and data for Franz Josef (Walker and Syers, 1976). In Fig. 5 we see how P, once released from its geologic source, is converted into less available (P-occluded) forms or is lost from the terrestrial system. With no more input of primary mineral  $P_w$ ,  $P_d$  the steady-state depends only on exogenous input. The  $P_v$ ,  $P_o$ , and  $P_d$  pools reach their steady-states of 5, 15 and  $0.02 \text{ g P m}^{-2}$  respectively, shortly after the  $P_w$  disappears, while the  $M_m$  and  $P_c$  pools reach their trivial steady-state only after about five hundred thousand years.

### 3.2.2 The Hawaii chronosequence

The Hawaiian archipelago, located in the North Pacific Ocean, is part of the Hawaiian-Emperor Ocean Mountain Range formed by hotspot volcanism moving in a southeast direction (Steinberger et al., 2004). This movement creates an island-age-gradient, which provides a perfect scenario to define a chronosequence. Hotspot volcanism forms the islands in a progressive way, while climate acts by weathering the fresh exposed rock and together with the topographical gradient, acts to enhance soil erosion.

317

To model the P dynamics of these islands, we consider the start of the model simulation shortly after the formation of the island. The initial  $P_w$  pool represents the total amount of P in fresh rock material left by the volcanic activity. For the simulation, we assume 2 m of rock material to account for the large pool of primary mineral left after the formation of the island. As the hotspot moves, there is no more uplift of material, and therefore we run the simulation with no uplift (i.e.,  $l_w = 0$ ). Hawaii receives very low P atmospheric input (Crews et al., 1995). Refer to Tables 2 and 3 for the parameters used for the simulation. Figure 6 shows the simulation results condensing them in three P pools:  $P_o$ ,  $P_c$ , and  $P_w$ , which are also the pools that Crews et al. (1995) considered in their analysis of the Hawaii chronosequence for the top 50 cm of soil.

Our simulations shows a general agreement with Crews et al. (1995) data. Both systems start with a large pool of  $P_w$ , although our initial pool is much larger, as we consider all the weatherable P in 2 m of basaltic rock and not only the top 50 cm. Productivity peaks at ca. 50 000 a and at ca. 100 000 a as the  $P_w$  is depleted, after which the ecosystem depends only on  $l_d$ . As the soil evolves the external P losses decrease, but another consequence of soil development is the formation of  $M_m$  increasing occlusion capacity, which results in a peak of  $P_c$  almost coinciding with the end of the  $P_w$  pool.

It should be noted that the decay in the P-organic pool may be delayed by P de-occlusion (ecosystems can invest carbon to de-occlude P) at the expense of the P-occluded pool. This fact may also act as a P-storage mechanism which delays the approach to steady state. However, in the long run, lateral erosion provides  $P_c$  and  $M_m$  losses which ultimately lead to a steady-state of the system after more than 100 000 a.

### 3.2.3 Dynamics of an uplift dominated site (the Amazon Basin)

In contrast with the P dynamics for the subducting part of two colliding plates (Franz Josef chronosequence) and the hotspot volcanism in the ocean crust forming the Emperor-Hawaiian Mountain Range (Hawaii chronosequence), continental crust dynamics differ due to the lower material crust densities which allow the crust to float on

318

the magma. To represent ecosystem dynamics on continental crust in a system that is relatively stable, we assume constant uplift rates. Figure 7 presents the dynamics of an ecosystem with very slow uplift rates, high soil moisture, and low exogenous inputs, similar to the ones reported for the various places in the Amazon Basin. The parameters used for the simulation are reported in Tables 2 and 3.

The system slowly reaches a steady-state in which the soil process still play an important role and the P-occluded is large compared to the P-organic. The system quickly recycles the organic matter, due to high temperatures and soil moisture conditions. This leads to stronger fluxes between the soil and the vegetation. This behavior contrasts to the observational data and modeled results for Hawaii and for Franz Josef. Stable continental crust reaches a steady-state in which the soils are constantly regenerated due to the erosion-uplift balance. Therefore, even in steady-state, secondary minerals ( $M_m$ ) represent a P sink to the system, as they are also constantly formed and eroded away. The slow uplift rates results in a system in which the two inputs  $I_w$  and  $I_d$  play an important role.

#### 4 Summary and conclusions

In this article we examined the effects of tectonic processes and exogenous inputs on the P-cycle. We have shown how steady states of productivity depend on exogenous inputs for systems that do not feature uplift such as terrestrial ecosystems on oceanic crust or systems experiencing subduction. We have also shown how the steady-state is not immediately reached after the primary mineral is depleted but after the occluding minerals are stabilized (not accounting for further losses of P). We contrasted this to ecosystems on continental stable crust where P occlusion and weathering play important roles in the transient as well as in the steady-state productivity of the ecosystems.

Hydroclimatic conditions, which are assumed to be constant, determine how fast ecosystems reach their steady-state (Walker and Syers, 1976), with humid ecosystems reaching this steady-state faster. This was well reproduced by our model, which

319

also showed that steady-state wet ecosystems generally run on a lower P budget because the P losses increase with soil moisture, while the inputs remain constant. This suggests that humid climates are not only P depleted because they reach their steady state faster, as proposed by Walker and Syers (1976), but also because they have a lower P budget, due to larger steady-state losses. Finally, in the case of low atmospheric and tectonic P inputs, ecosystems may rely on mechanisms to overcome P losses, such as the reduction of organic losses, increased P inputs from animals and vegetation symbiotic relations with mycorrhizae.

In summary, our simple dynamical system helps answer some of the complicated questions related to the origins and conditions of P limitation and how ecosystems may influence the P cycle in order to maintain P available for further growth. Moreover, we believe that the model simplicity and applicability to regional and global dynamics may not only help advance our understanding of the P-cycle, but also its coupling to other models of biogeochemical processes.

This model reproduces observations relatively well indicating that the important processes describing the terrestrial P dynamics are captured. The next step will be to implement this model into a global vegetation model, allowing it to represent climatic and tectonic forcing more explicitly. This will then allow us to quantify the importance of the P dynamics for terrestrial productivity, as well as the implications of P limitation for the response of terrestrial ecosystems to the different aspects of global change.

*Acknowledgements.* C.B. would like to thank the Biospheric theory and modeling group, Primăvara Grigoriu and Álvaro Buendía for the stimulating discussion and comments. A.P. was supported acknowledges the US National Science Foundation under grants EAR-0628432 and EAR-0635787, a collaboration grant from the US Department of Agriculture, Agricultural Research Service, Temple, TX and the support of the Landolt & Cie Chair "Innovative strategies for a sustainable future" at the École Polytechnique Fédérale de Lausanne, Lausanne, Switzerland.

The service charges for this open access publication have been covered by the Max Planck Society.

320

## References

- Artaxo, P. and Hansson, H.: Size distribution of biogenic aerosol particles from the Amazon Basin, *Atmos. Environ.*, 29, 393–402, 1994. 314
- Brady, N. C. and Weil, R. R.: *The Nature and Properties of Soil*, Prentice Hall, 13 edn., 2008. 303, 306, 307, 308, 309, 310, 315, 327
- Chadwick, O. A., Derry, L. A., Vitousek, P. M., Huebert, B. J., and Hedin, L.: Changing sources of nutrients during four million years of ecosystem development, *Nature*, 397, 491–497, 1999. 302, 304
- Chameides, W. L. and Perdue, E. M.: *Biogeochemical Cycles: A Computer-Interactive Study of Earth System Science and Global Change*, Oxford University Press, 1997. 307
- Cramer, W., Bondeau, A., Woodward, F., Prentice, I., Betts, R., Brovkin, V., Cox, P., Fisher, V., Foley, J., Friend, A., Kucharik, C., Lomas, M., Ramankutty, N., Sitch, S., Smith, B., White, A., and Young-Molling, C.: Global response of terrestrial ecosystem structure and function to CO<sub>2</sub> and climate change: results from six dynamic global vegetation models, *Global Change Biol.*, 7, 357–373, 2001. 304
- Crews, T., Kitayama, K., Fownes, J., and Riley, R.: Changes in soil phosphorus fractions and ecosystem dynamics across a long chronosequence in Hawaii, *Ecology*, 75, 1407–1424, 1995. 302, 304, 316, 318, 326
- Hughes, J. D.: Conservation in the Inca empire, *Capitalism Nature Socialism*, 10, 69–76, doi:10.1080/10455759909358886, 1999. 304
- Hungate, B. A., Dukes, J. S., Shaw, M. R., Luo, Y., and Field, C. B.: Nitrogen and Climate Change, *Science*, 302, 1512–1513, 2003. 304
- Kronberg, B., Fyfe, W., Leonardos, O., and Santos, A.: The chemistry of some Brazilian soils: Element mobility during intense weathering, *Chem. Geology*, 24, 211–229, 1979. 326
- Lasaga, A.: The kinetic treatment of geochemical cycles, *Geochimica et Cosmochimica Acta*, 44, 815–828, 1980. 304
- Mahowald, N. M., Artaxo, P., Baker, A. R., Jickells, T. D., Okin, G. S., Randerson, J. T., and Townsend, A. R.: Impacts of biomass burning emissions and land use change on Amazonian atmospheric phosphorus cycling and deposition, *Global Biogeochem. Cycles*, 19, GB4030.1–GB4030.15 doi:10.1029/2005GB002541, 2005. 303, 310, 326
- Mahowald, N. M., Jickells, T. D., Baker, A. R., Artaxo, P., Benitez-Nelson, C. R., Bergametti, G., Bond, T. C., Chen, Y., Cohen, D. D., Herut, B., Kubilay, N., Losno, R., Luo, C., Maen-
- haut, W., McGee, K. A., Okin, G. S., Siefert, R. L., and Tsukuda, S.: Global distribution of atmospheric phosphorus sources, concentrations and deposition rates, and anthropogenic impacts, *Global Biogeochem. Cycles*, 22, GB4026, doi:10.1029/2008GB003240, 2008. 303
- Manzoni, S., Porporato, A., D'Odorico, P., Laio, F., and Rodriguez-Iturbe, I.: Soil nutrient cycles as a nonlinear dynamical system, *Nonlin. Processes Geophys.*, 11, 589–598, 2004, <http://www.nonlin-processes-geophys.net/11/589/2004/>. 304
- Manzoni, S., Trofymow, J. A., Jackson, R. B., and Porporato, A.: Stoichiometric controls on carbon, nitrogen, and phosphorus dynamics in decomposing litter, *Ecological Monographs*, in press, 2010. 309
- McGroddy, M., Daufresne, T., and Hedin, L.: Scaling of C : N : P stoichiometry in forests worldwide: Implications of terrestrial redfield-type ratios, *Ecology*, 85, 2390–2401, 2004. 309
- Newman, E.: Phosphorus inputs to terrestrial ecosystems, *J. Ecology*, 83, 713–726, 1995. 306, 327
- Okin, G. S., Mahowald, N., Chadwick, O. A., and Artaxo, P.: Impact of desert dust on the biogeochemistry of phosphorus in terrestrial ecosystems, *Global Biogeochem. Cycles*, 18, GB2005, doi:10.1029/2003GB002145, 2004. 314, 326
- Porder, S., Vitousek, P. M., Chadwick, O. A., Chamberlain, C. P., and Hilley, G. E.: Uplift, Erosion and Phosphorus limitation in Terrestrial Ecosystems, *Ecosystems*, 10, 158–170, 2007. 303, 307, 308, 317, 326, 327
- Porporato, A., D'Odorico, P., Laio, F., and Rodriguez-Iturbe, I.: Hydrologic controls on soil carbon and nitrogen cycles. I. Modeling scheme, *Adv. Water Resour.*, 11, 589–598, 2004. 306, 308, 309, 325
- Rodriguez-Iturbe, I. and Porporato, A.: *Ecohydrology of water-controlled ecosystems: soil moisture and plant dynamics*, Cambridge Univ. Press, 2004. 310
- Steinberger, B., Sutherland, R., and O'Connell, R. J.: Prediction of Emperor-Hawaii seamount locations from a revised model of global plate motion and mantle flow, *Nature*, 430, 167–173, 2004. 317
- Stevens, P. and Walker, T. W.: Chronosequence concept and soil formation, *The Quart. Rev. Biology*, 45, 333–350, 1970. 303
- Strogatz, S. H.: *Nonlinear Dynamics and Chaos: With Applications to physics, Biology, Chemistry, and Engineering*, Cambridge, MA: Perseus Books, 1994. 304
- Tippett, J. and Kamp, P. J. J.: The role of faulting in rock uplift in the Southern Alps, New Zealand, *New Zealand Journal of Geology and Geophysics*, 36, 497–504, 2003. 317

- Walker, T. W. and Syers, J.: The fate of phosphorous during pedogenesis, *Geoderma*, 15, 1–19, 1976. 302, 303, 315, 316, 317, 319, 320, 325, 326
- Wardle, D. A.: Ecosystem Properties and Forest Decline in Contrasting Long-Term Chronosequences, *Science*, 305, 509–513, doi:10.1126/science.1098778, 2004. 302
- 5 Wardle, D. A., Bellingham, P. J., Bonner, K. I., and Mulder, C. P. H.: Indirect effects of invasive predators on litter decomposition and nutrient resorption on seabird-dominated islands, *Ecology*, 90, 452–464, 2009. 302, 304, 306, 307
- Zaehle, S., Friend, A. D., Friedlingstein, P., Dentener, F., Peylin, P., and Schulz, M.: Carbon and nitrogen cycle dynamics in the O-CN land surface model, II: The role of the nitrogen cycle in the historical terrestrial C balance, *Global Biogeochem. Cycles*, doi:10.1029/2009GB003522, in press, 2010. 304
- 10

323

**Table 1.** Description of symbols.

	Symbol	Description	Units
pools	$P_w$	phosphorus in primary material in the soil	$\text{g P m}^{-2}$
	$M_m$	secondary minerals	$\text{g M m}^{-2}$
	$P_c$	phosphorus occluded in secondary minerals	$\text{g P m}^{-2}$
	$P_v$	phosphorus in vegetation	$\text{g P m}^{-2}$
	$P_o$	phosphorus in soil biomass	$\text{g P m}^{-2}$
	$P_d$	phosphorus in soil solution	$\text{g P m}^{-2}$
fluxes	$F_{wd}$	phosphorus weathering	$\text{g P m}^{-2}$
	$F_{wm}$	secondary mineral formation	$\text{g P m}^{-2}$
	$F_{dc}$	phosphorus occlusion	$\text{g P m}^{-2}$
	$F_{dv}$	phosphorus uptake by vegetation	$\text{g P m}^{-2}$
	$F_{vo}$	phosphorus losses from vegetation	$\text{g P m}^{-2}$
	$F_{od}$	phosphorus mineralization	$\text{g P m}^{-2}$
losses	$O_m$	secondary minerals	$\text{g P m}^{-2}$
	$O_o$	phosphorus in organic form	$\text{g P m}^{-2}$
	$O_c$	phosphorus in occluded form	$\text{g P m}^{-2}$
	$O_d$	phosphorus in soil solution	$\text{g P m}^{-2}$
inputs	$I_d$	phosphorus in dissolvable form transported by atmosphere and animals	$\text{g P m}^{-2}$
	$I_w$	phosphorus supplied by uplift	$\text{g P m}^{-2}$

324

**Table 2.** Description of model parameters.

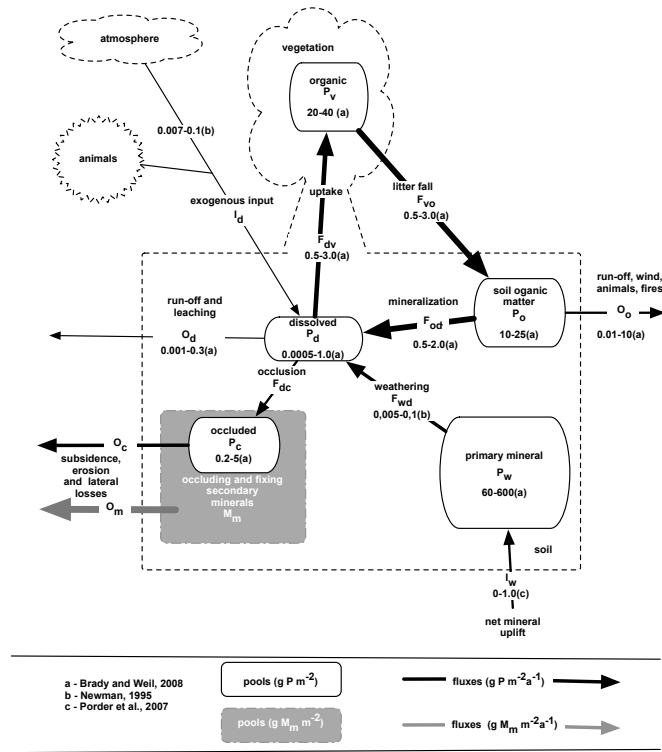
Parameter	Description	Value	Units	Reference
$s$	averaged soil moisture	2–8	dimensionless	Porporato et al. (2003)
$\eta$	maximum transpiration rate	5	mm m <sup>-2</sup> day <sup>-1</sup>	Porporato et al. (2003)
$Z_r$	effective soil depth	1	m	chosen value
$n$	porosity	0.4	dimensionless	chosen value
$k_w$	weathering rate	0.00021/ $Z_r$	a <sup>-1</sup>	calculated for Franz Josef data (Walker and Syers, 1976)
$k_m$	secondary mineral formation rate	0.7	a <sup>-1</sup>	chosen value
$k_c$	phosphorus occlusion rate	0.00005	a <sup>-1</sup>	chosen value
$k_e$	ice, wind and gravitational driven losses	0.00001	a <sup>-1</sup>	chosen value
$k_l$	runoff/leakage rate at saturation	0.1	a <sup>-1</sup>	Porporato et al. (2003)
$k_d$	mineralization rate	0.18615	a <sup>-1</sup>	chosen value
$k_v$	litter fall rate	0.20075	a <sup>-1</sup>	chosen value
$k_r$	losses regulation rate	0.002	a <sup>-1</sup>	see steady-state solution
$k_u$	active uptake by vegetation	10	dimensionless	see steady-state solution
$k_f$	ice, wind, human, fire losses rate	0.0005	a <sup>-1</sup>	see steady-state solution

325

**Table 3.** Parameter description for specific simulations.

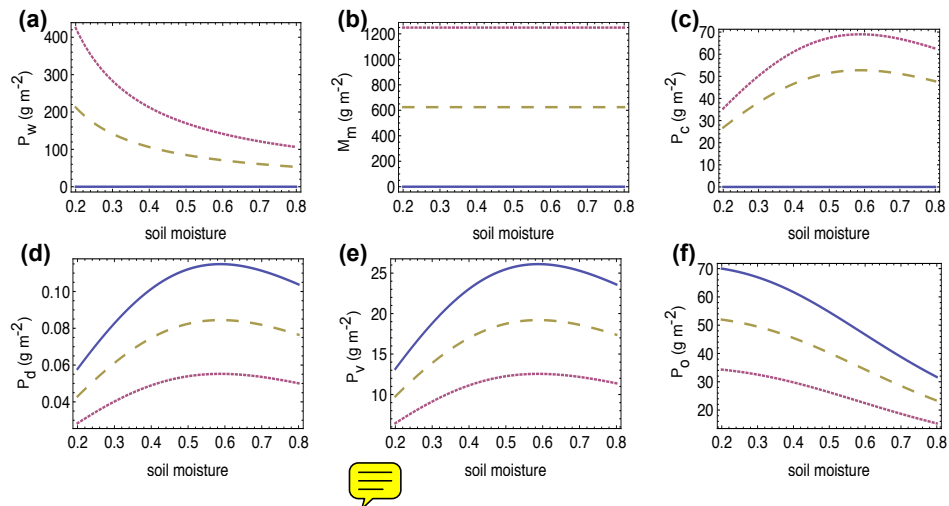
Parameter	Units	Franz Josef	Hawaii	Amazon Basin
tectonic uplift rate	mm <sup>-1</sup> a <sup>-1</sup>	0	0	0.0057 (Kronberg et al., 1979)
P in rock	mol m <sup>-3</sup>	38 (Porder et al., 2007)	200 (Crews et al., 1995)	100 (chosen value)
atmospheric input	g m <sup>-2</sup> a <sup>-1</sup>	0.01 (Walker and Syers, 1976)	0.001 (Okin et al., 2004)	0.00048 (Mahowald et al., 2005)
$k_{cl}$	a <sup>-1</sup>	0.7	0.5	0.7
$T$	°C	11	16	25
$s$		0.7	0.5	0.6

326



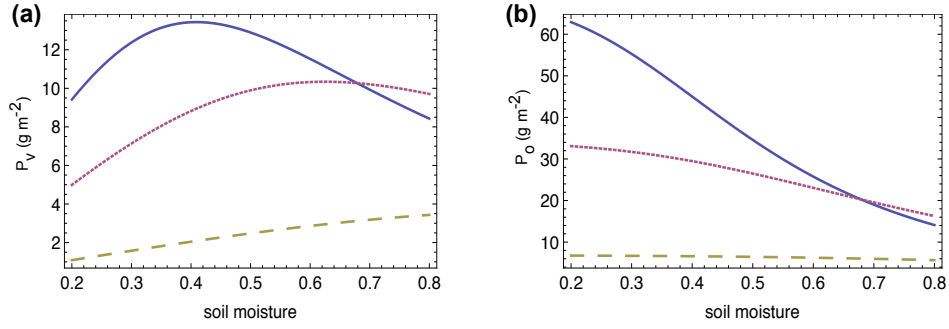
**Fig. 1.** Schematic representation of the terrestrial phosphorus cycle as described mathematically using Eqs. (12–17). Sizes of the fluxes and pools are taken from the literature Brady and Weil (2008); Porder et al. (2007); Newman (1995). The thickness of the arrows relates to the size of the fluxes.

327



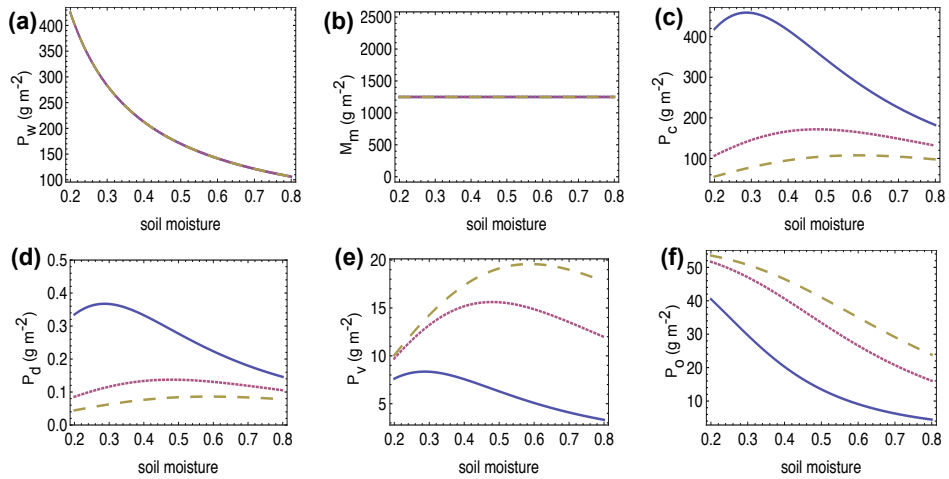
**Fig. 2.** Sensitivity of P external input to soil moisture. The dotted lines represent ecosystems depending only on uplift ( $I_w$ ), the solid lines represent ecosystem depending only on exogenous input ( $I_d$ ) and the dashed lines represent ecosystems depending on both,  $I_w$  and  $I_d$ . For these simulations we used the steady-state solution, where five P pools in steady state are shown in: (a) P primary mineral  $P_w$  Eq. (18), (c) P occluded  $P_c$  Eq. (20), (d) P dissolved in soil solution Eq. (23), (e) P in vegetation Eq. (22), and (f) P in soil organic matter Eq. (21). The pool of secondary minerals in steady state is presented in (b) Eq. (19). Refer to Table 2 for the parameters used.

328



**Fig. 3.** Sensitivity of organic biomass losses to soil moisture. For ecosystems in steady-state, we compare the effect of soil moisture on three different schemes of P in organic biomass losses ( $O_o$ ). The dashed line represents ecosystems with organic matter losses that are mainly driven by water. The solid line presents ecosystems with organic matter losses mainly driven by wind, human biomass removal and fires ( $k_f$ ) and the dotted line represents ecosystems with losses by both,  $k_f$  and  $k_r$ . Panel (a) illustrates the steady state for P in vegetation Eq. (22) and panel (b) represents the P in soil organic biomass Eq. (21). For this simulation we used  $l_d = l_w = 0.0045 \text{ g P m}^{-2} \text{ a}^{-1}$  and the values in Table 2.

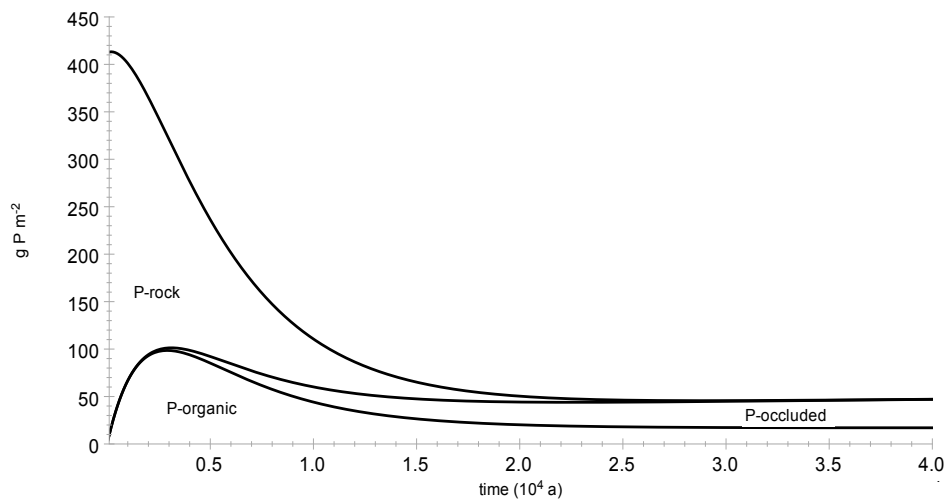
329



**Fig. 4.** Active P vegetation uptake ( $k_u$ ) sensitivity to soil moisture. To compare the result of the symbiotic relationship within ecosystems we simulated ecosystems with different uptake rates: the dotted lines represent no symbiosis ( $k_u = 1$ ), the solid lines represent strong symbiosis ( $k_u = 10$ ), and the dashed lines represent intermediate symbiosis ( $k_u = 5$ ). For these simulations, we used the steady-state solution, where five P pools in steady-state are shown in: (a) P primary mineral  $P_w$  Eq. (18), (c) P occluded  $P_c$  Eq. (20), (d) P dissolved in soil solution Eq. (23), (e) P in vegetation Eq. (22), and (f) P in soil organic matter Eq. (21). The pool of secondary minerals in steady state is presented in (b) Eq. (19). For the parameters used refer to Table 2 and to the system input parameters for the Amazon Basin in Table 3.

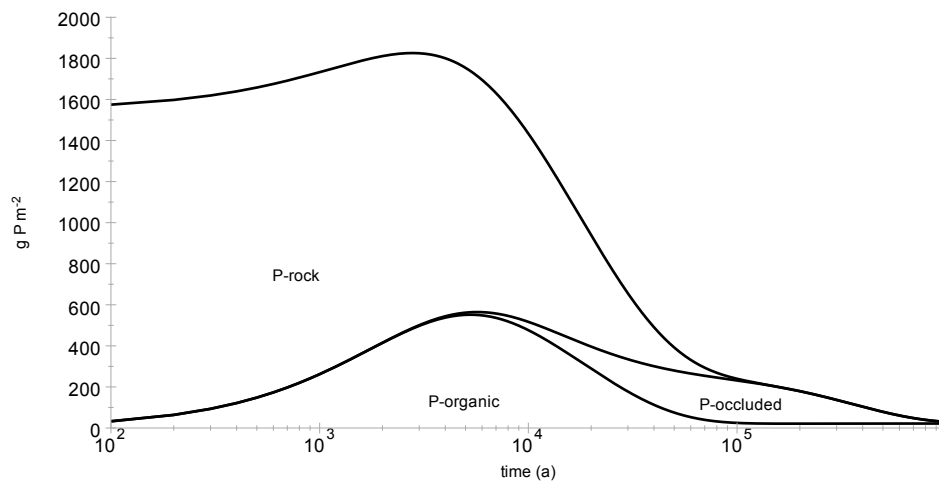
330





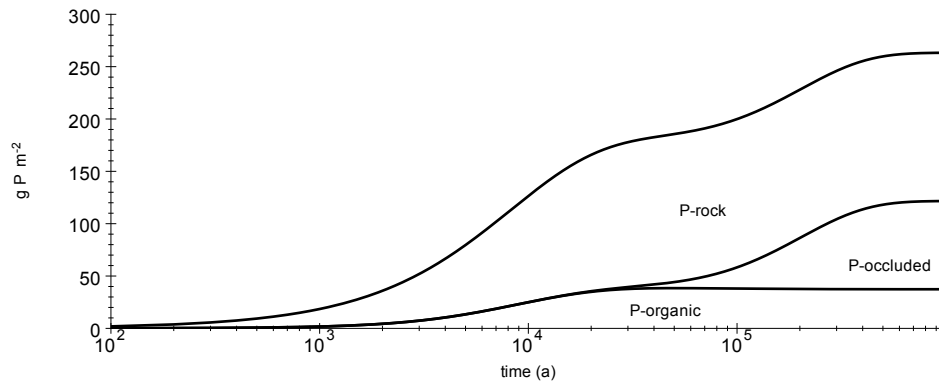
**Fig. 5.** Modeled phosphorus dynamics for the Franz Josef chronosequence. The areas between the lines represents the different P pools in the soil: P-rock ( $P_w$ ), P-organic ( $P_o + P_v + P_d$ ), and P-occluded ( $P_c$ ). The values of the parameters used for this model run can be found in Tables 2 and 3.

331



**Fig. 6.** P temporal dynamics for an ecosystem large initial P in rock pool. Simulated phosphorus transformation in time are shown using the parameters for Hawaii. The values of the parameters used for this model run can be found in Tables 2 and 3. The areas between the lines represent the sizes of the pools: P-rock (showing 25% of total  $P_w$ ), P-occluded ( $P_c$ ), and P-organic ( $P_o + P_v + P_d$ ). The values of the parameters used for this model run can be found in Tables 2 and 3. Note that the x-axis is plotted on a logarithmic scale.

332



**Fig. 7.** Modelled P dynamics for an ecosystem with slow uplift rates. This simulation uses the climate and atmospheric input for the Amazon Basin. The areas between the lines represents the different P pools in the soil: P-rock ( $P_w$ ), P-organic ( $P_o + P_d + P_v$ ), and P-occluded ( $P_c$ ). The values of the parameters used for this model run can be found in Tables 2 and 3. Note that the x-axis is plotted on a logarithmic scale.